A new chapter in the never ending story of cycloadditions: the puzzling case of SO_2 and acetylene.

Zoi Salta[a*], Oscar N. Ventura[b], Nadjib Rais[a, c], Nicola Tasinato[a] and Vincenzo Barone[d]

[a] *Scuola Normale Superiore, piazza dei Cavalieri 7, 56126 Pisa, Italy*
[b] *Computational Chemistry and Biology Group, CCBG, DETEMA, Facultad de Química, Universidad de la República, 11400 Montevideo, Uruguay*
[c] *IUSS Scuola Universitaria Superiore, Piazza della Vittoria 15, 27100 Pavia, Italy*
[d] *INSTM, via G. Giusti 9, 50121 Firenze, Italy*

Abstract: A comprehensive study of the different classes of cycloaddition reactions ([3+2], [2+2] and [2+1]) of SO_2 to acetylene and ethylene has been performed using density functional theory (DFT) and composite wavefunction methods. The [3+2] cycloaddition reaction, that was previously explored in the context of the cycloaddition of thioformaldehyde S-methylide (TSM) to ethylene and acetylene, proceeds in a concerted way to the formation of stable heterocycles. In this paper we extend our study to the [2+2] and [2+1] cycloadditions of SO_2 to acetylene, which would produce 1,1-oxathiete-2-oxide and thiirene-1,1-dioxide respectively. One of the main conclusions is that cyclic 1,1-oxathiete-2-oxide can open through a relatively easy breaking of the S-O single bond and rearrange toward sulfinyl acetaldehyde (SA). The SA molecule can easily undergo several internal rearrangements, which eventually lead to sulfenic acid and sulfoxide derivatives of ethenone, 1,2,3-dioxathiole, and CO plus sulfinylmethane. The most probable path, however, produces 2-thioxoacetic acid, whose derivatives (or those of the corresponding acetate) are usually obtained by Willgerodt–Kindler-type sulfuration of acetates. This product can in turn decompose, leading to the final products CO_2 and $H_2C{=}S$. Comparison of this decomposition path with that of 2-amino-2-thioxoacetic acid shows that the process occurs through different H-transfer processes.

Keywords: [2+2], reaction mechanism, DFT, reduced-cost composite methods, cyclic compounds.

***Corresponding author:** Dr. Zoi Salta, Scuola Normale Superiore, piazza dei Cavalieri 7, 56126 Pisa, Italy, E-mail: Zoi.Salta@sns.it

1. INTRODUCTION

The intricate subject of cycloaddition reactions, including their mechanisms and potential synthetic applications, is an ongoing and widely debated topic in the literature. Cycloaddition reactions are widely employed in organic synthesis to produce cyclic compounds possessing specific stereochemistry and functional groups. Their applications cover diverse fields including medicinal chemistry, materials science, and the synthesis of natural products. [1] Despite a large number of experimental and theoretical studies, some mechanistic aspects deserve further investigation. For example, the widely studied and utilized Diels – Alder [4+2] cycloaddition reaction has recently been found to compete with the [2+2] cycloaddition. [2,3]

In a previous paper,[4] we investigated the [3+2] cycloaddition of O_3 (ozone), SO_2 (sulfur dioxide), CH_2OO (formaldehyde oxide, Criegee radical), CH_2SO (sulfine) and CH_2SCH_2 (thioformaldehyde S-methylide) to ethylene and acetylene, in order to understand how the mechanism of pericyclic processes, like 1,3-dipolar cycloadditions, is influenced not only by the nature of the substituents, but also by the kind and number of heteroatoms in the 1,3-dipole. In this work, we extend the investigation to all the reaction steps involved in the different types of cycloaddition reactions between sulfur dioxide and acetylene. A comparison with the corresponding reactions of SO_2 with ethylene is also carried out. Besides the [3+2] cycloadditions already studied,[4] which produce 1,3,2-dioxathiolane (1A) and 1,3,2-dioxathiole (2A) respectively, other possible reactions are the [2+2] and [2+1] cycloadditions, which lead respectively to 1,2-oxathietane 2-oxide (1B) and thiirane 1,1-dioxide (1C) in the case of ethylene, and 1,2-oxathiete 2-oxide (2B) and thiirene 1,1-dioxide (2C) in the case of acetylene. The three addition mechanisms are shown in Figures 1(a) for ethylene and 1(b) for acetylene, where 1 is assigned to ethylene and 2 to acetylene, while A, B, and C identify the [3+2], [2+2] and [2+1] cycloadditions, respectively. Notice that the same limiting resonance structures shown in Scheme 1 for sulfur dioxide can also describe ozone[6], but their relative weights are different in the two compounds. Formulas including lone pairs were added below each of the resonant structures.

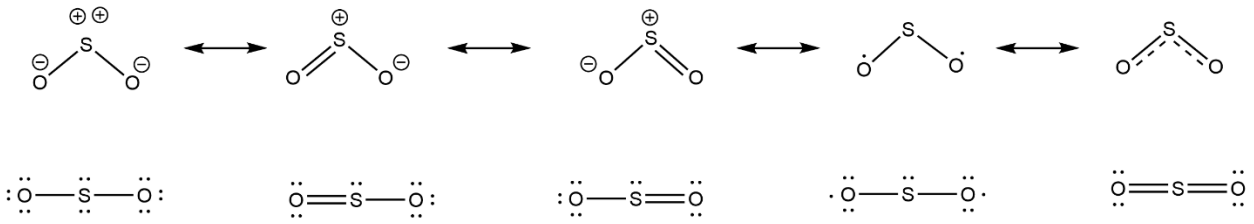

Scheme 1. Resonant structures of SO_2.

In particular, the last structure, which implies the involvement of the *d*-orbitals of the central atom in the bonds with the terminal atoms, has a negligible importance for ozone. The interested reader is directed to the paper by Lan, Wheeler and Houk[6] for a further detailed comparison of the orbitals of O_3 and SO_2 in their [3+2] cycloaddition to ethylene and acetylene.

To the best of our knowledge, only two papers have been devoted to 2A, one by Liebman et al.[5] in the context of the study of cyclic sulfites and sulfates (respectively the *S*-oxide and *S,S*-dioxide of 1,3,2-dioxathiolane) and another one by Lan et al.[6] in the context of the comparison of O_3 and SO_2 [3+2] cycloaddition to ethylene and acetylene (both 1A and 2A). We were not able to find any experimental report on the structure of 2A in the literature, and neither theoretical nor experimental studies on 2B have been published. In the case of 2C, also known as ethylene episulfone, several papers have been published (especially concerning its carbon substituted derivatives, like dimethylthiirene dioxide),[7,8] but it seems that no information (neither experimental nor theoretical) concerning the reactivity patterns and possible end-products of the species involved in the cycloaddition reaction of SO_2 to ethylene and acetylene is yet available.

Our first goal in this work is to analyze the three possible mechanisms from the point of view of stability of the products 2A, 2B, and 2C, in the reaction with acetylene, but most importantly from the point of view of the feasibility of such reactions. A comparison with the corresponding reactions for ethylene is also performed.

Our second purpose is to investigate whether some of the primary products of the cycloadditions can suffer internal reorganization and further reaction, and, if so, to determine the structure and energetics of all possible intermediates, transition states and products on these reaction paths. In this respect, 1,2-oxathiete 2-oxide (2B) turned out to be the most interesting species, since the thioester O–S bond can be broken quite easily. A similar process in the product of the reaction with ethylene, 1B, is not feasible, because of the lack of a C=C bond that explains the richness of isomerization paths for 2B, as we will see in the following sections of this study.

Finally, the controversial issue of the preference for a concerted or non-concerted mechanism of the [3+2] cycloaddition of SO_2 to acetylene, was reinvestigated by a large panel of theoretical methods. The results provided by the most accurate methods confirmed the preference for a concerted reaction mechanism ruled by a symmetric transition state.

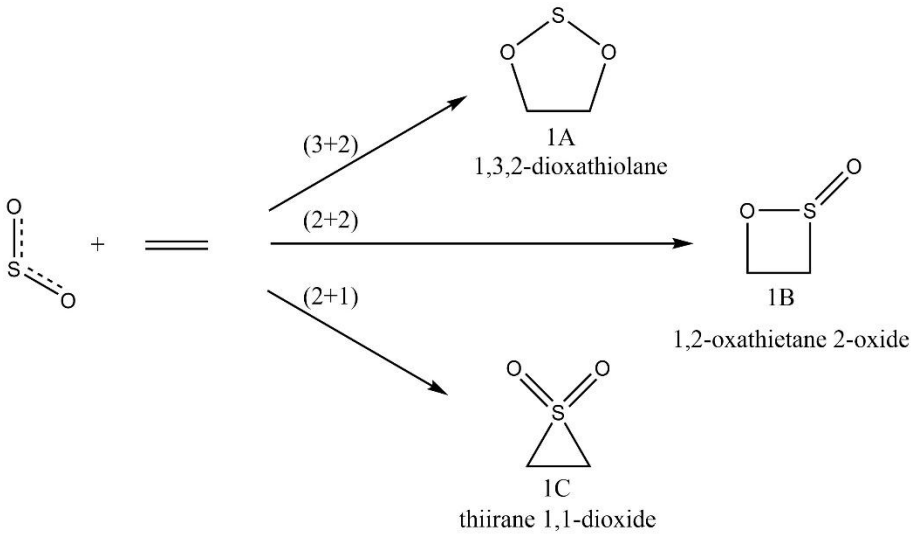

Figure 1(a). Possible cycloaddition products for the reaction of SO_2 with ethylene.

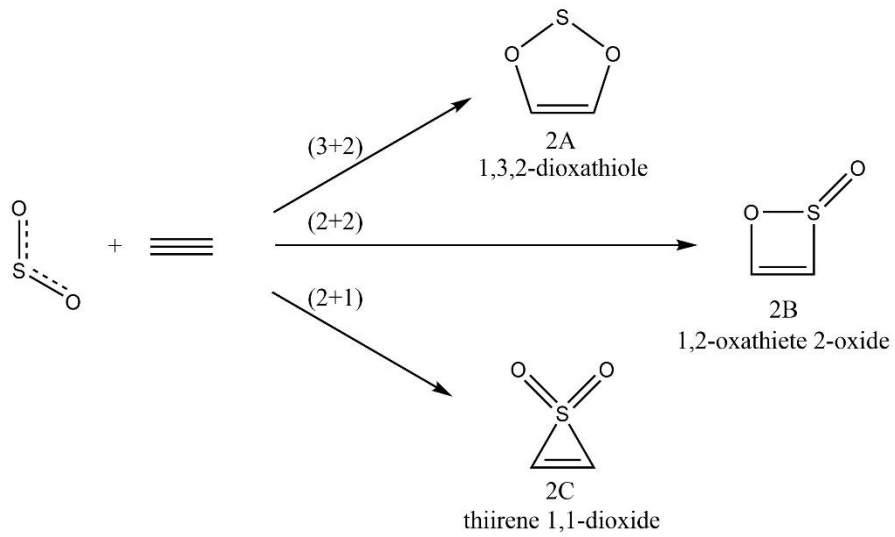

Figure 1(b). Possible cycloaddition products for the reaction of SO_2 with acetylene.

2. COMPUTATIONAL DETAILS

Based on previous experience[4], we used Density Functional Theory (DFT) and wavefunction-based composite methods to obtain optimized geometries, frequencies, energies, and thermochemical properties of the different species. The latter were calculated using standard statistical thermodynamics formulas within the rigid rotor/harmonic oscillator (RRHO) approximation. A low-level investigation of the Potential Energy Surfaces (PESs) of each reaction was performed using the fast CBS-QB3[9,10] composite method, which relies on the B3LYP[11] hybrid functional for geometry optimizations. More sophisticated thermochemical calculations were performed using the W1BD[12-14] and jun-Cheap (jChS)[15-17] composite methods, which rely respectively on B3LYP and revDSD-PBEP86[18] density functionals to determine optimized geometries and frequencies, and on single-point energy evaluations at those geometries by the Brückner doubles ansatz[19], or a combination of complete basis set (CBS)[20] – MP2[21] and CCSD(T)[22] approaches – to estimate accurate energies. In the case of the TS2A transition state, hybrid M06-2X[23] and double hybrid DSD-PBEP86[24] and B2PLYP[25] density functionals were used, as well as explicitly correlated MP2-F12[26] and CCSD(T)-F12[27] methods. DFT methods were combined with different Dunning[28,29] and Weigend−Ahlrichs[30] basis sets, and augmented by Grimme's DFT-D3 dispersion contribution. [31] In order

to improve the description of the computed properties, Dunning's basis sets were augmented by an additional set of *d* functions on the sulfur atom. [32,33] The same basis sets were used in conventional wavefunction methods, whereas cc-pVnZ-F12 basis sets[34-36] were used in explicitly correlated computations.

Geometry optimizations were carried out at first and then, on the optimized geometries, the determination of the Hessian matrix was performed, and the eigenvalues were analyzed for the absence of negative values for minima or the presence of only one negative value in the case of the transition states. Harmonic frequencies were then used to evaluate the zero-point vibrational energy (ZPE). Intrinsic Reaction Coordinate (IRC[37]) calculations were performed to verify that the transition states obtained connect the correct reactants and products on the different reaction paths. Atomic charges and bond densities were determined using Weinhold's Natural Bond Orbital (NBO) analysis.[38] All DFT and composite methods calculations presented in this paper were performed using Gaussian 16, Revision C.01,[39] while optimizations at the CCSD(T), CCSD(T)-F12 and MP2-F12 levels of theory were done using the Molpro2020[40] package.

3. RESULTS AND DISCUSSION

3.1. [2+2] and [2+1] addition of SO_2 to ethylene and acetylene

The [2+2] reaction of SO_2 with ethylene would produce 1,2-oxathietane 2-oxide (also known as β-sultine, a cyclic ester of sulfinic acid, 1B), whose derivative with phenyl and methyl substituents was isolated and characterized by Durst and Gimbarzevsky[41,42] and also studied as a key intermediate for obtaining other compounds by Breau et al.[43] A more recent review on sultines was published by Bondarenko et al.[44] Very few experimental studies are available for cyclic sultines and computational investigations are completely lacking.

Similarly, the [2+1] reaction of SO_2 with ethylene would produce the parent ethylene episulfone 1C. The first preparation of episulfones from episulfides was reported by Johnson and Taylor in 1997[45], and

more recently an efficient synthesis of episulfones was published by Harel et al.[46] An accurate geometrical structure of 1C was obtained from microwave spectroscopy and compared with several other compounds, including dimethyl sulfone[47].

On the other hand, experimental or recent theoretical studies are lacking for the reactions with acetylene. A single old paper by Hase et al.[48] was found, where the authors used CNDO/S and Hartree-Fock calculations to explore conjugative and inductive group effects on derivatives of cyclopropene and included thiirene-1,1-dioxide, 2C. Unfortunately, the level of theory of these results is completely inadequate for the current standards of quantum chemical computations. The geometries of the four species 1B, 1C, 2B and 2C optimized at different levels of theory are shown in Figure 2 and the corresponding relative ground state energies, enthalpies and free energies, are collected in Table 1.

Table 1. Relative energies with respect to reactants, for the products of the three possible cycloadditions of SO_2 to ethylene and acetylene. All the values are in kcal mol^{-1}. Enthalpies and free energies are reported at T=298.15 K.

Ethylene	1A: [3+2]			1B: [2+2]			1C: [2+1]		
	Δ(E+ZPE)	ΔH	ΔG	Δ(E+ZPE)	ΔH	ΔG	Δ(E+ZPE)	ΔH	ΔG
CBS-QB3	17.9	16.5	29.1	11.3	10.1	22.3	22.0	20.7	33.6
revDSD/jun(T+*d*)	18.1	16.6	29.1	9.8	8.5	20.6	20.3	18.8	31.5
W1BD	18.8	17.4	29.3	11.2	10.0	21.5	21.4	20.0	32.1
jChS	18.6	17.1	29.6	11.1	9.8	21.9	21.2	19.8	32.4
Acetylene	2A: [3+2]			2B: [2+2]			2C: [2+1]		
	Δ(E+ZPE)	ΔH	ΔG	Δ(E+ZPE)	ΔH	ΔG	Δ(E+ZPE)	ΔH	ΔG
CBS-QB3	8.7	7.2	18.3	3.2	1.9	12.7	26.1	24.7	35.8
revDSD/jun(T+*d*)	8.5	6.9	18.3	0.8	-0.6	10.5	24.8	23.3	34.6
W1BD	8.9	7.5	18.6	2.8	1.4	12.4	25.8	24.4	35.6
jChS	8.8	7.2	18.6	2.7	1.3	12.4	25.6	24.1	35.3

For a better understanding of the bonding patterns between the three different types of the SO_2-cycloaddition reactions with both ethylene and acetylene, NBO atomic charges for each atom of the species

in Figure 2 are displayed in a.u. Dipole moments as well as the charge distribution of the highest occupied molecular orbitals (HOMOs) of the stable species 1A-2C are also shown in the picture.

The first remarkable item is that the geometries optimized at the DFT and CCSD(T)-F12 levels are very similar, a feature that increases the confidence on the conclusions obtained from these calculations. In the second place, the increase of the dipole moments going from complexes A to complexes C, indicates an increase in the polarization of the species. In fact, looking to the charges on the sulfur and oxygen atoms, complexes A show approximately a (+1) charge on sulfur and (-1) charges on the oxygens, while complexes C exhibit an approximate (+2) charge on sulfur and (-1) on each oxygen. Meanwhile, complexes B exhibit an intermediate situation, where the oxygen bound exclusively to sulfur shows an approximate (-1) charge and the other oxygen a smaller charge. Furthermore, the C atoms of methylene groups evolve from a vanishing to a significantly negative (-0.6) charge. In fact, if one leaves aside the positively charged hydrogen atoms, the heavy atom structure of 1C closely resembles that of SO_2^{2-}. Finally, another remarkable observation is that the polarity of the molecules evolves in a different way for ethylene and for acetylene. While the dipole moment of 1A is larger than that of 2A, the opposite happens with 1C and 2C. Accordingly, 1A is less stable than 2A, but 2C is less stable than 1C (see Table 1). The situation with 1B and 2B is different and in both cases the B complexes are more stable than either the A or C species (see later on). This difference is also apparent in the distribution of the HOMO in the three species. Although some similarities can be found between the 1 and 2 complexes, there are very important differences connected with the presence of the double bond in the acetylene complexes.

The optimized structures of the four transition states for the [3+2], [2+2], and [2+1] reactions of SO_2 with ethylene and acetylene are also shown in Figure 2. Both an analysis of the bond distances and the charges show asymmetry of the addition, except in the case of TS1A and TS2A. A detailed discussion of this latter case is presented towards the end of this manuscript.

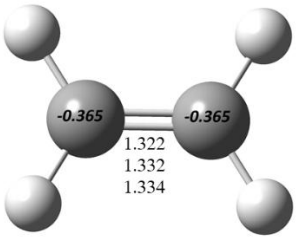

Ethylene

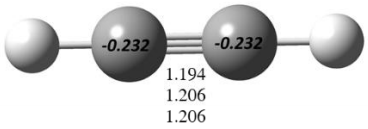

Acetylene

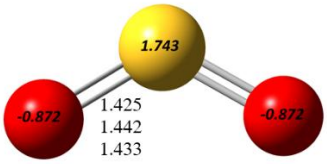

SO_2

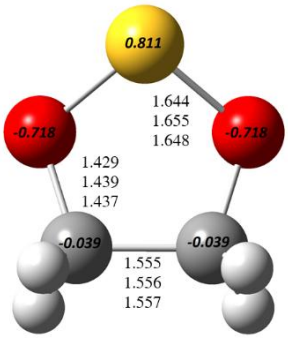

1A (μ = 2.7 D)

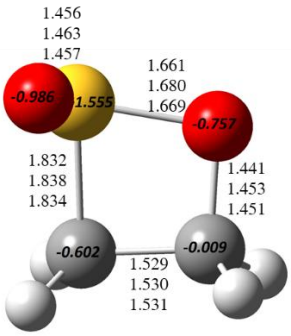

1B (μ = 4.4 D)

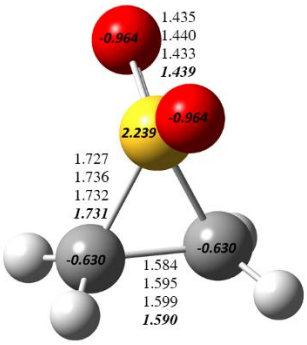

1C (μ = 4.9 D)

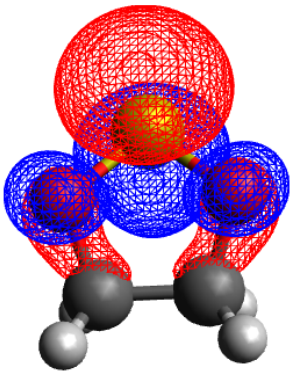

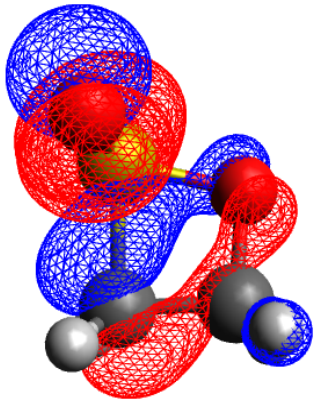

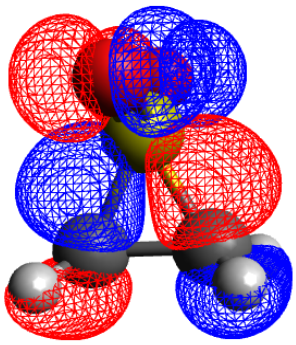

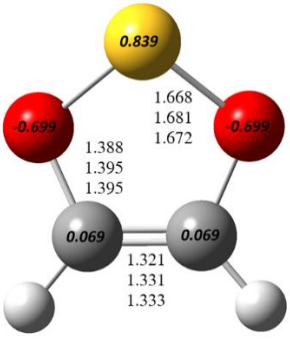

2A (μ = 1.8 D)

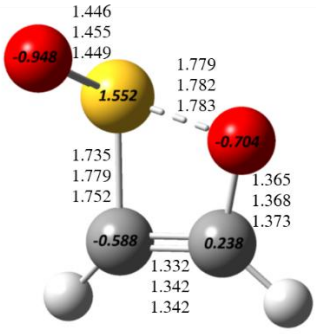

2B (μ = 4.1 D)

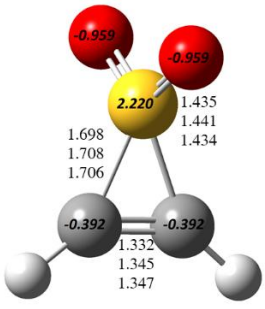

2C (μ = 5.4 D)

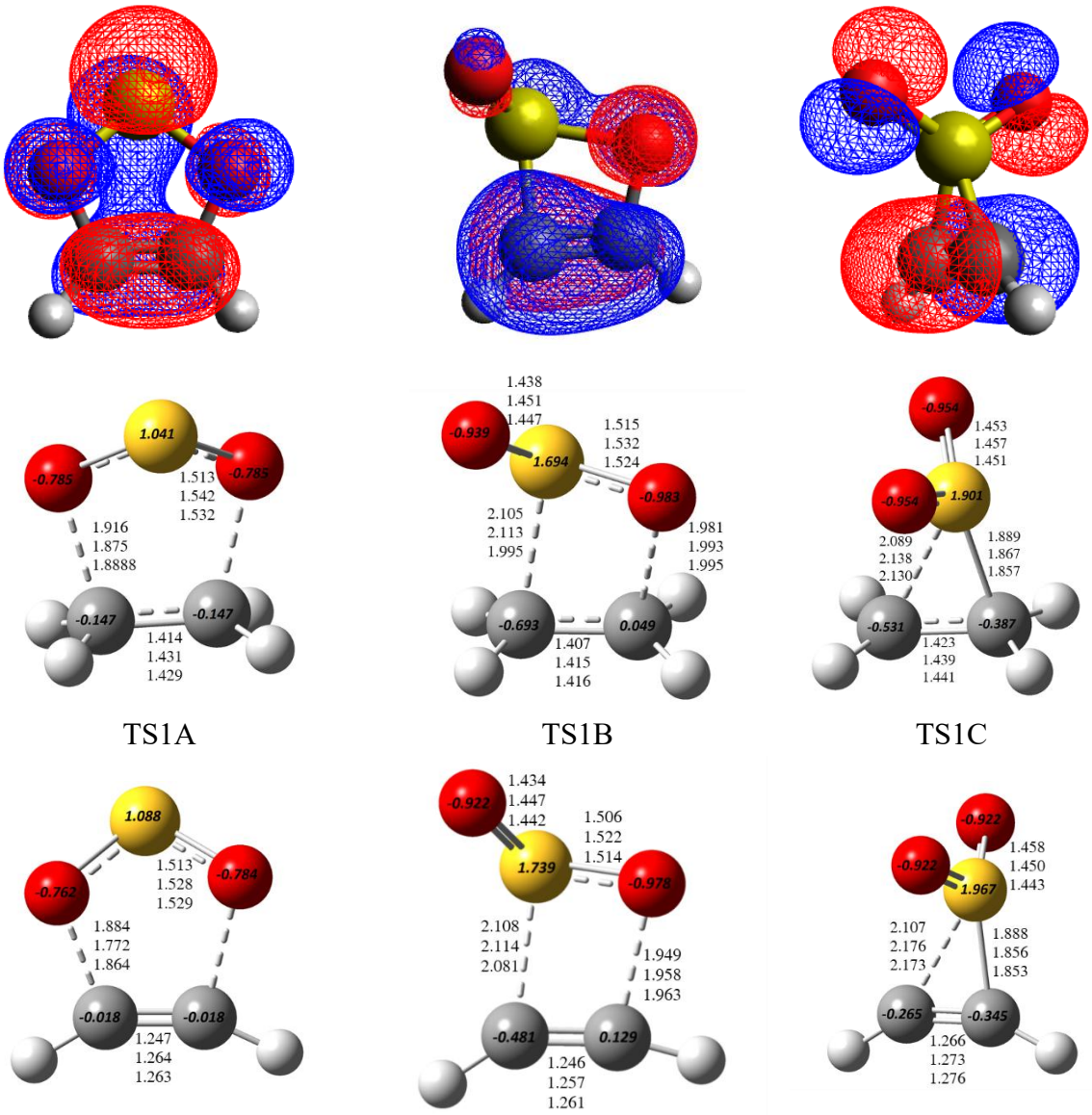

Figure 2. Structure of the minima and transition states of the [3+2], [2+2] and [2+1] cycloaddition reactions of SO_2 with ethylene and acetylene showing the most important bond distances (in Å). From top to bottom, M06-2X-D3/jun-cc-pV(T+*d*)Z, revDSD-PBEP86-D3(BJ)/jun-cc-pV(T+*d*)Z, and CCSD(T)-F12/cc-pVDZ-F12. For 1C, the experimental results taken from Ref. [47] are inserted as the 4th line. NBO charges calculated at the revDSD-PBEP86-D3(BJ)/jun-cc-pV(T+*d*)Z level and HOMO electronic distributions are presented.

The initial steps in the cycloaddition reactions of ethylene and acetylene with SO_2, including the relative Δ(E+ZPE) energies calculated at the jChS level, are sketched in Figures 3(a) and 3(b), respectively. It is apparent that the transition states for the three cycloadditions are quite high in energy and probably the

reactions are possible only at high temperatures. The TSs for the [2+2] cycloadditions are the lowest in energy and thus these reactions are the most likely to be achieved. Notice that even if the products for the same cycloaddition for ethylene and acetylene exhibit differences of several kcal mol^{-1}, the corresponding TSs are much more similar in energy. For example, while the energy difference between 1B and 2B is ~10 kcal mol^{-1}, the transition states TS1B and TS2B, are both 44 kcal mol^{-1} higher in energy than the corresponding reactants. In the case of acetylene, the product of the [3+2] addition 2A is not much more endothermic than 2B, (6 kcal mol^{-1} at the best level of calculation), but the barrier TS2A is 25% higher than TS2B. The barrier to obtain 2C is even larger than that necessary to obtain 2A, so we can discard also this species. If we assume that 44.4 kcal mol^{-1} had to be provided to achieve 2B, then neither 2A or 2C nor any of the derived products would be obtained, but saSA is clearly feasible both thermodynamically and kinetically. This aspect will be analyzed in more detail in the following.

A distortion/interaction energy analysis was carried out at this point to have a better understanding of the previous reactivity patterns. In the following Table 2, the electronic activation energy (ΔE_a), distortion energy (ΔE_d) of each of the fragments in the transition states and interaction energies (ΔE_i), with the latter being calculated as $\Delta E_i = \Delta E_a - \Delta E_d$, are presented.

Table 2. Activation (ΔE_a), distortion (ΔE_d) and interaction (ΔE_i) energies at the jChS level of theory. All values in kcal mol^{-1}.

	ΔE_a	**ΔE_d**				**ΔE_i**
TS		SO_2	Ethylene	Acetylene	Sum	
TS1A	49.9	25.4	24.3		49.7	0.2
TS1B	42.4	8.1	9.3		17.4	25.0
TS1C	50.4	1.3	9.6		10.9	39.5
TS2A	53.7	24.6		14.9	39.5	14.2
TS2B	43.0	6.8		12.0	18.8	24.2
TS2C	55.4	0.5		16.5	17.0	38.4

In both series, ethylene + SO_2 and acetylene + SO_2, the addition of the distortion energies of both fragments decreases in the order [3+2] > [2+2] > [2+1], while the opposite is true for the ΔE_i. Thus, the most probable reason as to why TS1B and TS2B exhibit the lowest activation energy in each series is

because of the equilibrium between the decreasing deformation energy and the increasing interaction energy of the deformed fragments. Another interesting observation is that the major contribution to the distortion energy comes mainly from ethylene or acetylene, and not from sulfur dioxide, with the most obvious example being the [2+1] cycloaddition of acetylene.

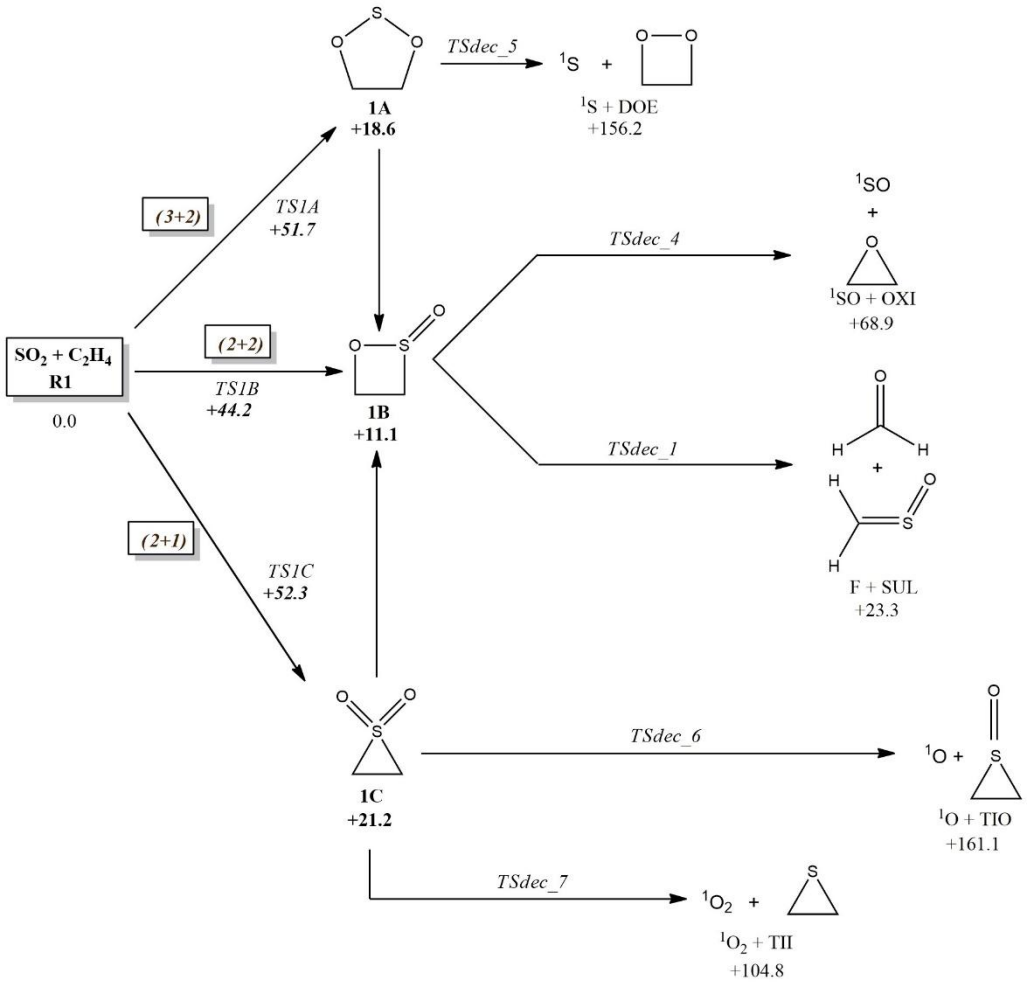

Figure 3(a). Scheme of the initial steps in the cycloaddition reactions of ethylene with SO_2. Relative Δ(E+ZPE) energies at the jChS level are included.

The situation is similar for the reaction with ethylene. 1B is the least unstable of the initial products and its decomposition would give rise to even less stable species. Even if probably closed under ordinary

experimental conditions (because the combined energy of these products is higher than those of both 1A and 1C) it is interesting that there exists a reaction channel that would lead to the formation of formaldehyde and sulfine. We did not consider important, however, to investigate further this reaction in this work.

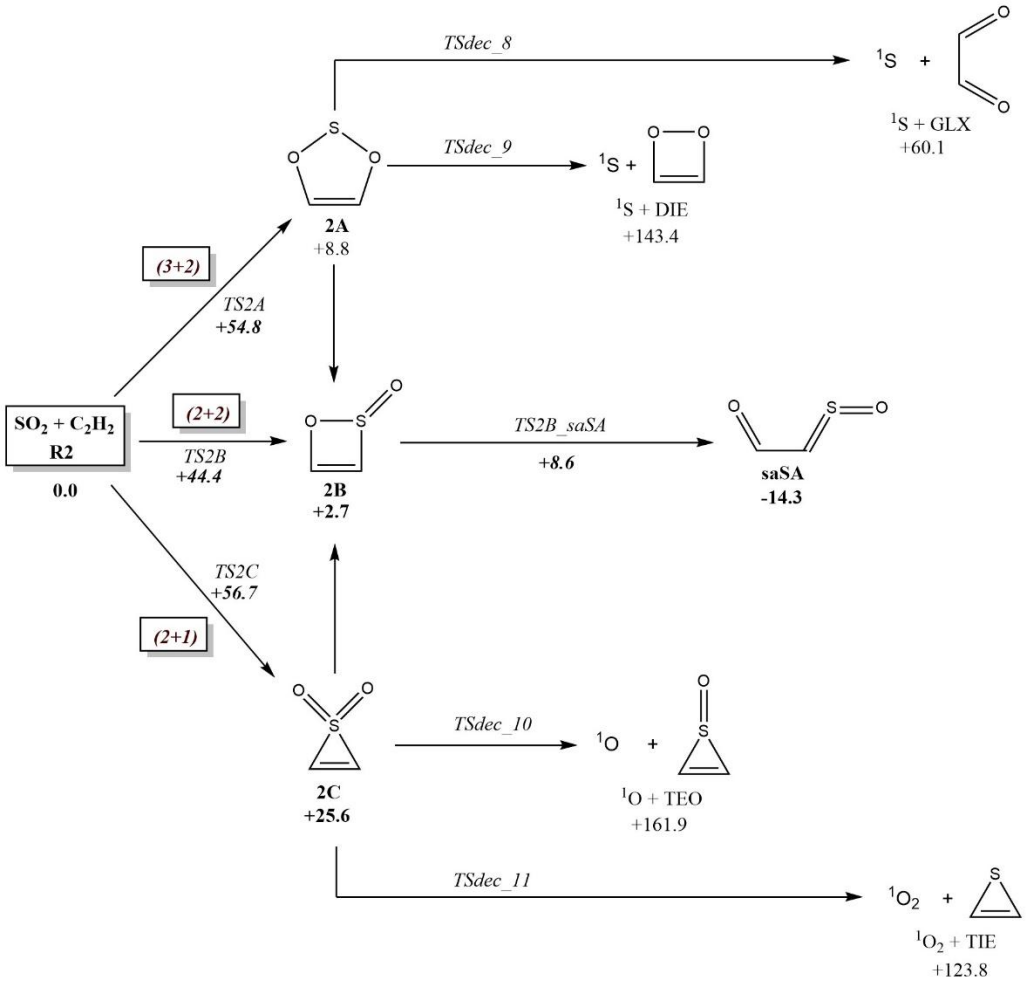

Figure 3(b). Scheme of the initial steps in the cycloaddition reactions of acetylene with SO_2. Relative Δ(E+ZPE) energies at the jChS level are included.

The products of the reactions with acetylene are more interesting because of the presence of the C=C double bond. 2A could eventually give either *cis*-glyoxal (GLX) or the isomer 1,2-dioxethene (DIE), plus singlet elementary sulfur, in both cases several kcal mol^{-1} over 2A. 2C might eventually lose an oxygen

atom in the closed-shell excited state to give thiirene S-oxide (TEO), or similarly, a closed-shell oxygen molecule plus thiirene (TIE), but the reactions do not seem feasible since these products lie again at too high energies.

On the other side, 2B can evolve easily to the isomeric sulfinyl acetaldehyde (saSA, see later), since the barrier is very low in comparison to that needed to revert to 2B (5.9 vs. 41.7 kcal mol^{-1}). The most important feature is that saSA lies 14.3 kcal mol^{-1} below the reactants, and has a $\Delta G^o(298.15K)$ of –5.7 kcal mol^{-1} at the jChS level, which implies that the reaction from 2B to saSA is spontaneous. It represents thus a favorable path for the [2+2] cycloaddition of SO_2 to acetylene, and we analyze in the following section all the possible subsequent reactions.

3.2. The reactions of 1,2-oxathiete-2-oxide (2B)

As mentioned above, 2B can evolve easily to sulfinyl acetaldehyde (SA) with *syn* or *anti* conformations of the OCCS and CCSO dihedrals (saSA). The barrier at 0 K is only 5.9 kcal mol^{-1} and straightforward to overcome once the initial barrier over TS2B (44.4 kcal mol^{-1}) is successfully surmounted. The general scheme of the possible reaction paths starting from 2B is shown in Figure 4 and the potential energy surface PES obtained at the jChS level is shown in Figure 5. Relative ground state energies (Δ(E+ZPE), enthalpies (ΔH) and free energies (ΔG) of all the species involved in the PES are collected in Table S.1 of the supporting information.

There are four possible conformers for SA, *syn-anti*, *anti-anti*, *anti-syn* and *syn-syn* with similar stabilization energies, all of them below that of the reactants. The initial conformer saSA exhibits the second smallest $\Delta G^o(298.15K)$ in absolute terms (–5.6 kcal mol^{-1}), while the Gibbs free energies of the other three conformers are –3.8 (ssSA), –7.2 (aaSA) and –7.4 kcal mol^{-1} (asSA). As expected, the rotation of the acetyl group is much easier than the rearrangement of the sulfoxide group, the latter exhibiting much larger barriers, but still below that of TS2B. Barriers for all the conversions depicted in Fig. 4 are collected

in Table 3 at different levels of calculation. It is important to point out that, except for three transition states and one product, all the stable species and the transition states are below the energy of TS2B. Thus, if the system has enough energy to overcome this initial TS, most of the rest of the PES (see Fig. 5) is accessible without any extra energy cost. The breaking of the O–S bond in 2B leads to the saSA isomer, from which the acetyl group can easily rotate (overcoming a barrier of 5.1 kcal mol^{-1}) to produce spontaneously the aaSA conformer, about 2 kcal mol^{-1} more stable. Specifically, the difference in the standard Gibbs energy between the two conformers, namely $\Delta\Delta G^o(298.15K)$, amounts to –1.9 kcal mol^{-1}. The saSA isomer can alternatively give ssSA passing through the transition state TSiso_9 (see Fig. 6), which however is less favored than the rotation of the acetyl group. Indeed, the barrier is much larger than that over TSiso_1 to give ssSA (39.8 vs 5.1 kcal mol^{-1}) and the isomer is about 3 kcal mol^{-1} less stable. Moreover, in this case $\Delta\Delta G^o(298.15K)$ is positive though small, 1.8 kcal mol^{-1}, so that all these facts indicate that the reaction saSA → aaSA is more probable than saSA → ssSA. In spite of this advantage the barrier for this latter reaction, 39.8 kcal mol^{-1}, is still below the energy necessary to reach 2B, meaning that the transition state is submerged. In the case of the isomerization of aaSA to asSA the situation is different. The barrier is now much higher (51.5 kcal mol^{-1}), the isomers are almost isoenergetic and $\Delta\Delta G^o(298.15K)$ is very small (–0.1 kcal mol^{-1}).

Table 3. Energy barriers for each one of the important transformations shown in Figure 4. Δ(E+ZPE) energies are given in kcal mol^{-1}.

Reaction	Transition State	revDSD/jun-cc-pV(T+*d*)Z	CBS-QB3	W1BD	jChS
$R1^1$ → 1A	TS1A	50.5	50.0	52.8	51.7
$R1^1$ → 1B	TS1B	42.3	44.2	44.7	44.2
$R1^1$ → 1C	TS1C	58.0	52.6	53.1	52.3
$R2^2$ → 2A	TS2A	54.2	55.6	54.5	54.8
$R2^2$ → 2B	**TS2B**	**43.1**	**44.7**	**43.6**	**44.4**
$R2^2$ → 2C	TS2C	62.7	57.2	56.1	56.7
2B → saSA	TS2B_saSA	4.1	3.5	5.7	5.9
saSA → aaSA	TSiso_1	11.2	5.2	5.3	5.1
saSA → ssSA	TSiso_9	47.1	40.2	40.2	39.8
ssSA → 2A’	TSiso_10	71.0	61.0	61.7	61.2
ssSA → asSA	TSiso_4	3.1	3.3	3.6	2.0
asSA → ETP	TSiso_3	46.2	43.3	47.3	46.2

asSA → aaSA	TSiso_2	55.9	43.3	51.8	51.5
ETP → TOOt	TSiso_7	56.8	53.6	53.4	51.1
TOOt → TOOc	TSiso_7’	7.2	4.3	4.5	4.5
TOOc → OTO	TSiso_8	63.9	65.5	65.5	65.4
OTO → CO + SUL	TSdec_3	37.9	30.7	30.1	29.8
ETP → EOS	TSiso_6	51.9	38.6	56.2	56.3
ETP → TOA	TSiso_11	47.4	45.0	46.0	43.8
aaSA → asSA	TSiso_2	59.0	43.3	51.8	51.5
aaSA → EOS	TSiso_5	39.2	41.5	41.3	41.2
EOS → PTP	TSiso_12	40.8	42.0	41.5	43.1
EOS → ELS	TSiso_13	90.6	91.6	92.2	91.8
EOS → SO + H_2CCO	TSdec_2	45.2	38.8	38.8	38.5
TOA → CO_2 + H_2CS	TSdec_4	67.3	69.7	69.6	69.3

[1] R1 = SO_2 + ethylene; [2] R2 = SO_2 + acetylene

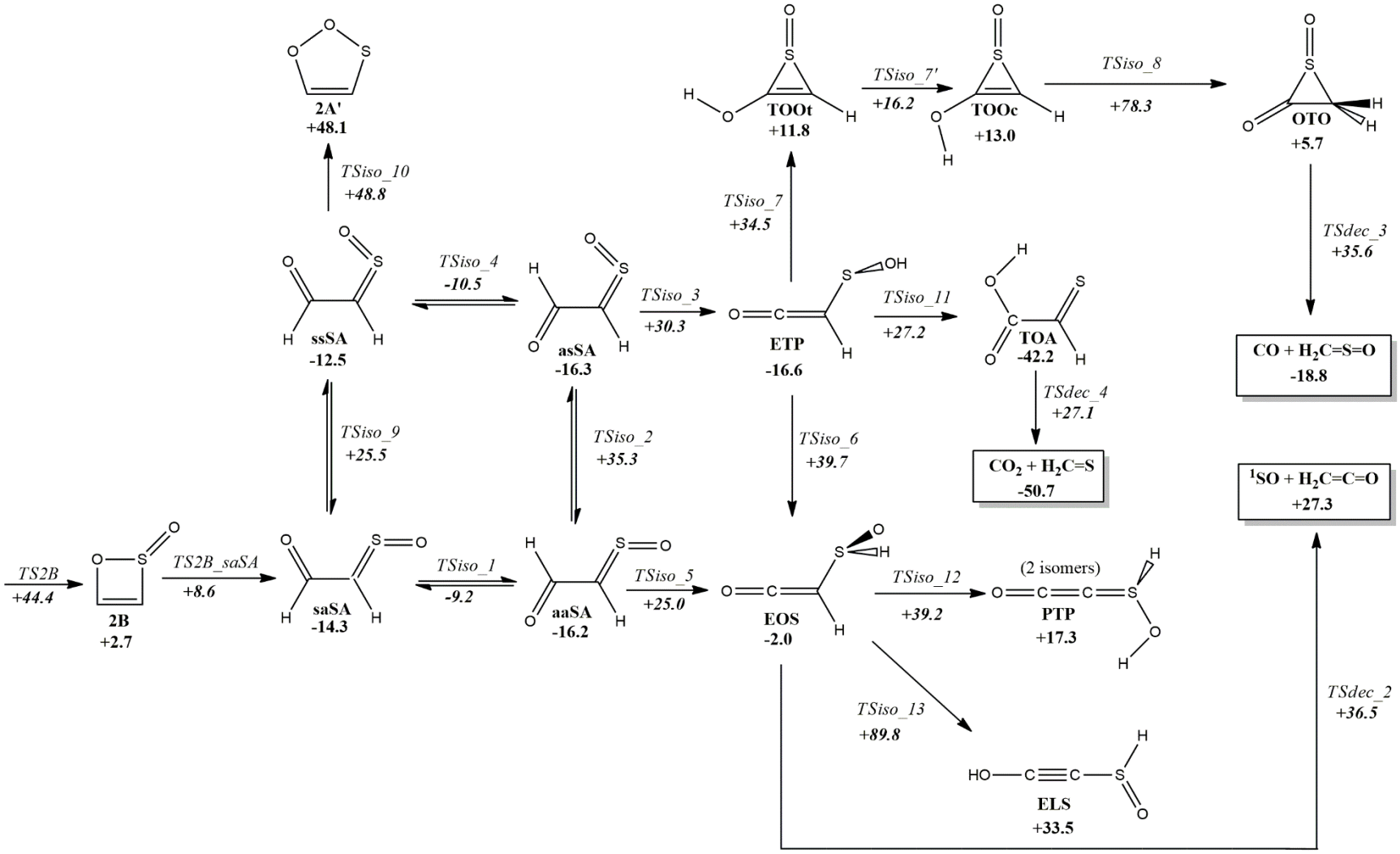

Figure 4. Isomerization paths of 2B. Relative Δ(E+ZPE) at the jChS level are shown in kcal mol^{-1}.

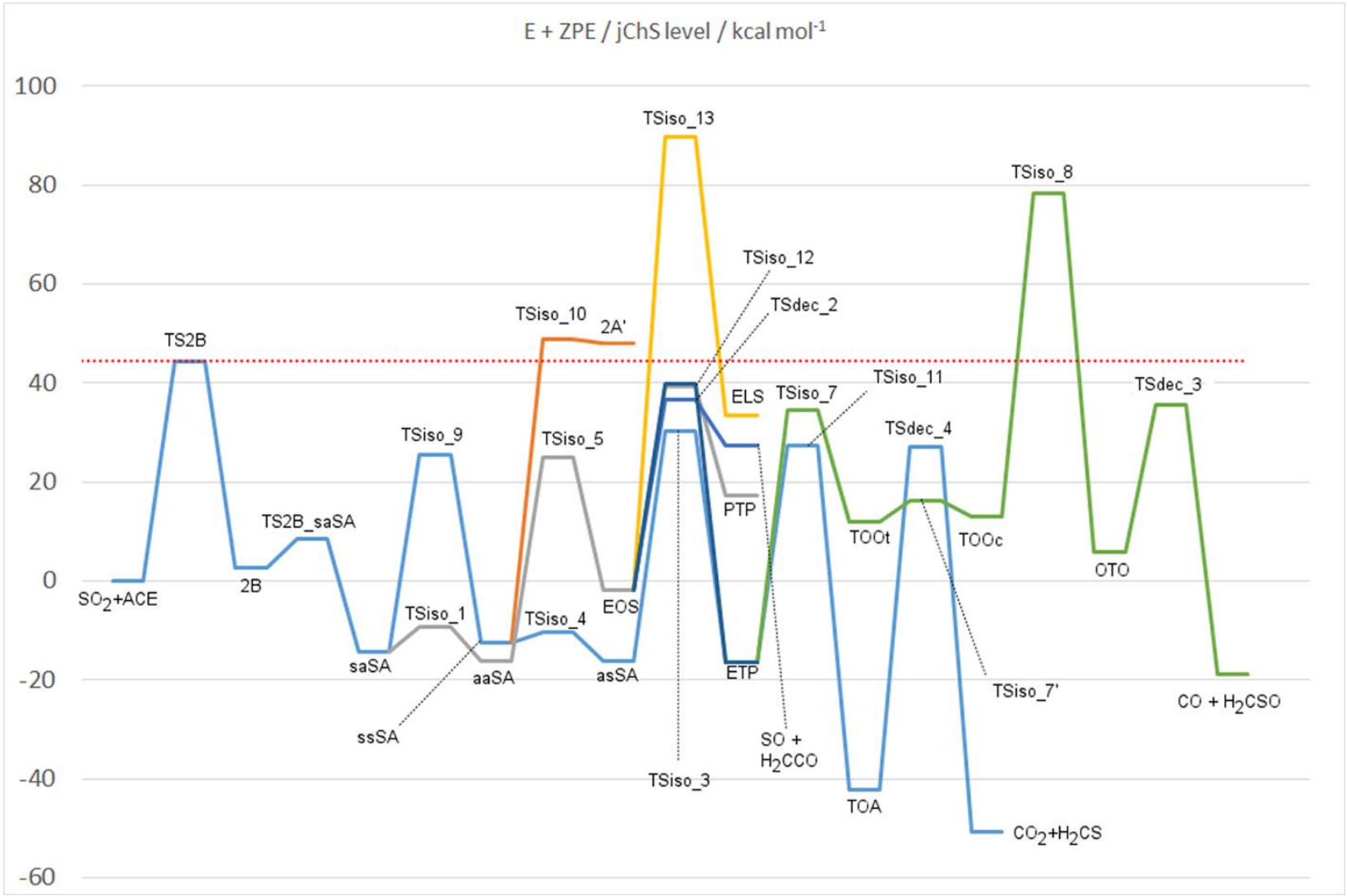

Figure 5. Potential energy surface, in kcal mol^{-1}, obtained at the jChS level (E+ZPE energies). The naming of the structures correspond to those in Figure 4 and Table 3. To help with the interpretation of the reaction paths, a dotted horizontal line was drawn at the energy of TS2B. ACE is an acronym for acetylene.

The fact that the barrier for the conversion over TSiso_9 is about 12 kcal mol^{-1} lower than that over TSiso_2, combined with the discussion in the previous paragraph, suggests that the equilibrium between the different conformers involves the circuit asSA ⇄ ssSA ⇄ saSA ⇄ aaSA, but not asSA ⇄ aaSA (i.e. TSiso_2 would hardly be overcome) with isomer asSA being the most stable at all temperatures. Notice again that the largest barrier in this possible circuit is for the isomerization saSA ⇄ ssSA over TSiso_9, at 39.8 kcal mol^{-1}, still lower than the energy needed to reach 2B. Therefore, the equilibrium of the four conformers can be taken for granted. The relative height of the transition states TSiso_9 and TSiso_2 shows that the *syn* conformation of the acetyl group helps the rearrangement of the C=S=O group.

To add some more information for the understanding of these interactions, we have included in Figure 6 the structures of all the conformers involved in the "circuit" mentioned above, and added also the NBO atomic charges in a.u. for the transition states connecting them.

The structure and most important geometrical parameters of the species not presented in the main text of this study, as well as, the Cartesian coordinates for all the species involved, are collected in Figure S.1. and Table S.2, respectively, in the Supporting Information.

The conformer ssSA is the least stable of the four isomers at all temperatures. Besides reversion to saSA (overcoming a barrier of 38.0 kcal mol^{-1}) or acetyl rotation to asSA (overcoming a much smaller barrier of 2.0 kcal mol^{-1}), one could think that a ring-closure through bonding of the terminal oxygen atoms is possible, with a concomitant reduction of S(IV) to S(II) and formation of a double bond between the carbon atoms. The resulting species 2A' is a structural conformer of 2A, not only much less stable, but also requiring a much higher reaction barrier of 61.3 kcal mol^{-1} to be obtained. On the contrary, the reverse barrier for the ring opening of 2A' is very small, the cycloreversion extremely probable, and almost certainly this product is not formed under any circumstances. It is one of the few TSs in the PES that is above the energy necessary to obtain 2B.

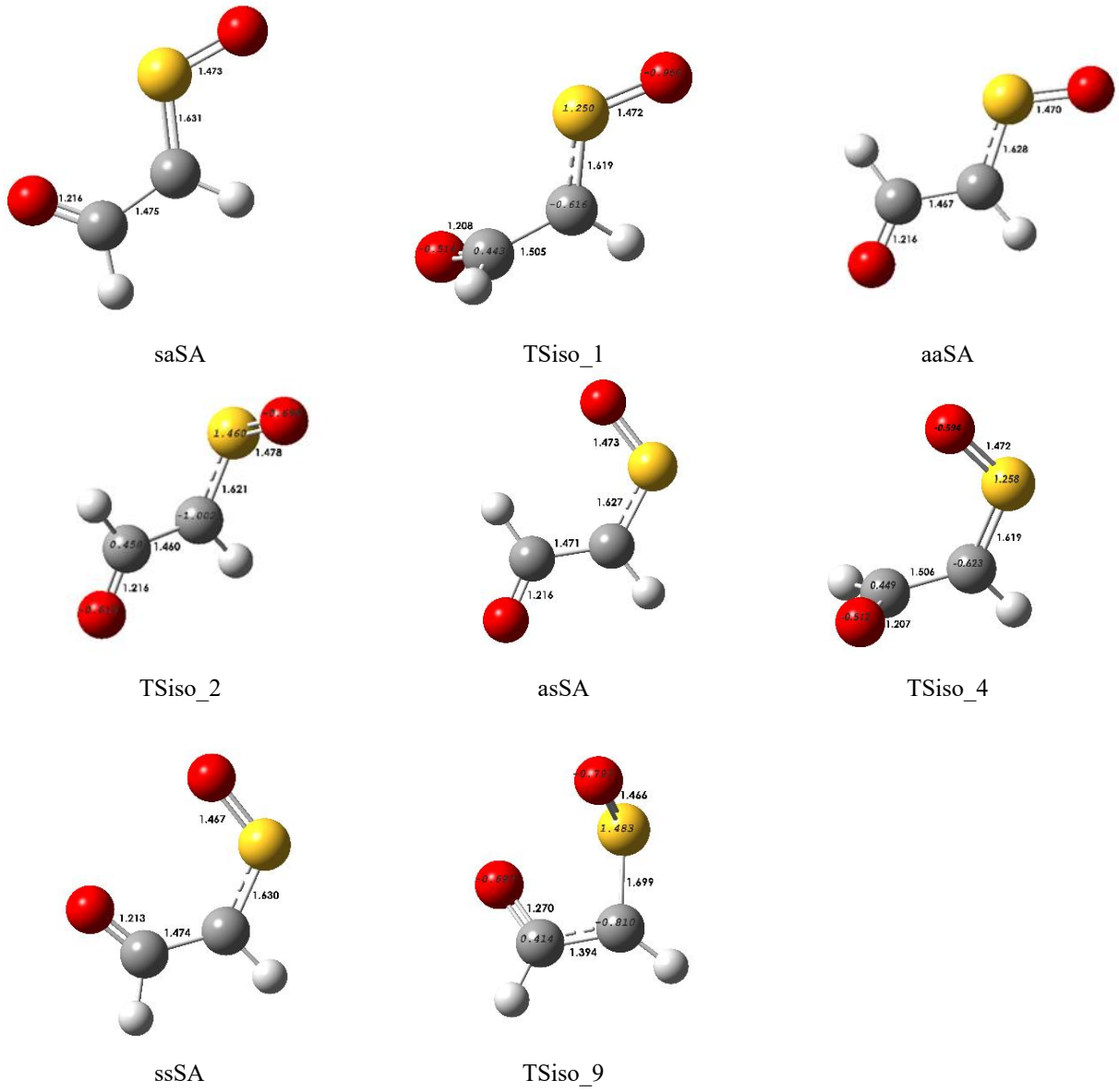

Figure 6. Structure of the SA conformers and transition states studied in this paper at the revDSD-PBEP86-D3(BJ)/jun-cc-pV(T+*d*)Z level. Most significant bond distances are given in Å. For the transition states, atomic charges (a.u.) from NBO analysis is also reported.

The asSA conformer is about 4 kcal mol^{-1} more stable than the ssSA intermediate at 0 K and about 2 kcal mol^{-1} more stable than the initial saSA isomer. The same relation occurs at 298.15 K if we use the free energies. The SA conformers are probably stable in vacuo or inert solvents in the absence of nucleophiles unless they suffer polymerization. Very few papers in the literature dealt even with α or β derivatives of SA[49,50], let alone the parent compound for which we did not find neither theoretical nor

experimental results. Several studies of sulfinyl ketones have been published however[54] and some mentions of sulfinyl acetaldehyde can be found concerning the mechanism of dissociation of hypotaurine from the cysteinsulfinate pathway by transamination. [52] Notice however that all these papers studied the sulfinyl group in a structure different from the one we are discussing in this paper, as shown in Scheme 2.

The α-sulfinylaldehydes studied in the literature were originally derived from methyl p-tolyl sulfoxide (MTS) which, as depicted in Scheme 2, may be represented as exhibiting a double or a dative bond between the sulfur and oxygen atoms. [53] We have recently analyzed the peculiarity of these bonding situations[54] in the context of a reassessment of the enthalpies of formation of some sulfenic acids. [55] The absence of R_2 in SA, as well as the toluene bound to the sulfur atom, made all the conformers of this species completely planar, and does not add a sulfur stereospecific center.

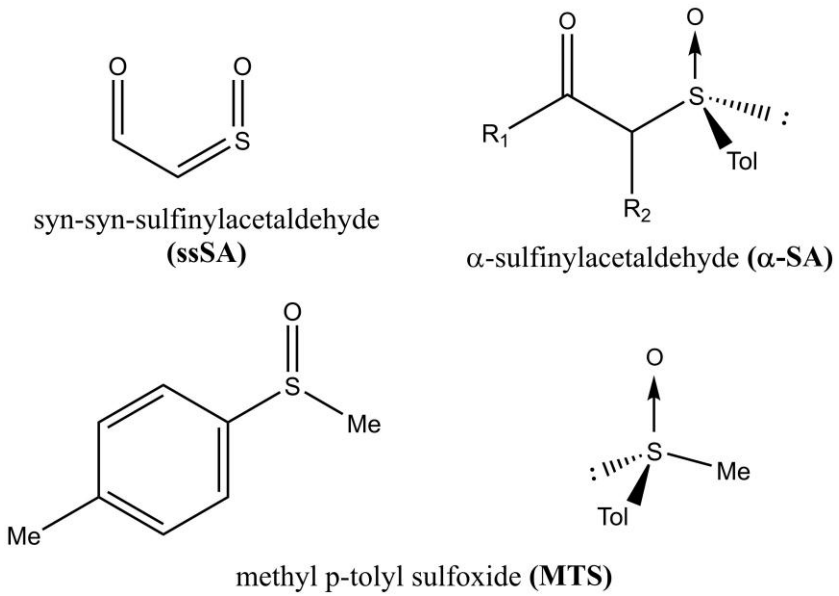

Scheme 2. Structure of sulfinyl acetaldehyde and sulfoxides studied in the literature and the sulfinyl acetaldehyde studied in this paper.

Even if asSA is the most stable conformer, all rotamers will be present and, in principle, they might be able to react further. We showed already that ssSA and saSA have few reactive possibilities, either the

reverse reactions or affording asSA and aaSA over smaller barriers. Thus, the important thing is to understand what happens with the reactions of these conformers.

The formation of asSA requires to overcome a barrier (E+ZPE) of 46.6 kcal mol^{-1}, slightly higher than that needed to obtain 2B, ending up with a small cumulene, ethenone 1-(SO)-thioperoxol, ETP, a species slightly more stable than asSA, which has further routes of transformation. This reaction would be spontaneous at room temperature since the free energy is –2.6 kcal mol^{-1} in favor of ETP. Two of the pathways, those leading to EOS (see later) and to the cyclic TOOt, TOOc and OTO species, which might decompose to CO plus sulfine (SUL), require significantly more energy than that necessary initially to obtain 2B, 56.3 and 51.1 kcal mol^{-1} respectively. Moreover, the transition state TSiso_8 is significantly higher than TS2B, requiring a hefty amount of energy. However, 2-thioxoacetic acid (TOA) can be reached over a lower transition state TSiso_11, with a total barrier of 43.8 kcal mol^{-1}, slightly smaller than that necessary to obtain 2B. TOA is around 42 kcal mol^{-1} more stable than the reactants, the reaction is spontaneous by almost 40 kcal mol^{-1} in ΔG, and may be considered the end product of this reaction path, except for the possibility of decomposition, as we will see later.

On the other side, the conformer aaSA can overcome TSiso_5 with a lower barrier of 41.2 kcal mol^{-1}, but the species obtained, ethenone (oxo)-λ^4-sulfane, EOS, is significantly less stable than the thioperoxol ETP. Furthermore, neither the isomerizations nor the decomposition give products which are over the reactants, so thermodynamically these are reactions less likely to occur than the obtention of TOA.

3.3. The structure of TOA and the influence of the substituents

The structure of the R-(C=S)-COOH species, R=H, CH_3, CH_3CH_2 and NH_2, is shown in Figure 7. There is no experimental or theoretical information on these species, except for R=NH_2, which was optimized at the B3LYP/6-311++G(3df,3pd) and CCSD(T)/cc-pVTZ levels of theory. [56] We have performed geometry optimizations at the DFT level, using the hybrid M06-2X-D3/jun-cc-pV(T+*d*)Z and double-hybrid revDSD-

PBEP86-D3(BJ)/jun-cc-pV(T+*d*)Z procedures, and used also the CCSD(T)-F12 post-Hartree-Fock explicitly correlated method to get a more precise idea of the structure of the parent species (TOA).

The modification of the substituent in the order R = H, NH_2, CH_3, CH_2CH_3 causes a small decrease in the angle C-C=O of about 3.5 degrees, and no significant variation in the C=O bond. The variation in the C-O, C-C and C=S bonds, however, is now different, with TOA and TOA_NH_2 exhibiting the shortest and longest C=O and C-C bonds, respectively. Because of these variations, the O-H···S hydrogen bond reaches its shortest value in TOA_NH_2, while it is 0.1 Å longer in TOA.

To make a comparison with the results by Bernhardt et al.[56] we calculated the reaction path for the transformation:

$$\text{R-(C=S)-COOH} \rightarrow \text{R-C-SH} + CO_2 \rightarrow \text{R-C(H)=S} + CO_2 \qquad (1)$$

with R = H and NH_2. Only the results at the revDSD-PBEP86-D3(BJ)/jun-cc-pV(T+*d*)Z and jChS levels are reported in this paper. A full in-depth study will be postponed for an ensuing publication, because the comparison of the possible reaction paths for different substituents requires a detailed study akin to that of Bernhardt et al.[56] including the calculation of rate coefficients at different temperatures.

Bernhardt et al.[56] found a reaction that followed the transformations shown in Scheme 3A. They actually studied the reverse reaction, the combination of aminomercaptomethylene (called 1t in their paper) with CO_2 to give 2-amino-2-thioxoacetic acid (TOA_NH_2), through a zwitterion that rearranges easily. The energy difference between 1t-CO_2 and TOA_NH_2 was found to be 20 kcal mol^{-1} at the CCSD(T)/cc-pVTZ level in their study. It was therefore appropriate to inquire whether a similar mechanism, Scheme 3B, would be operative for TOA.

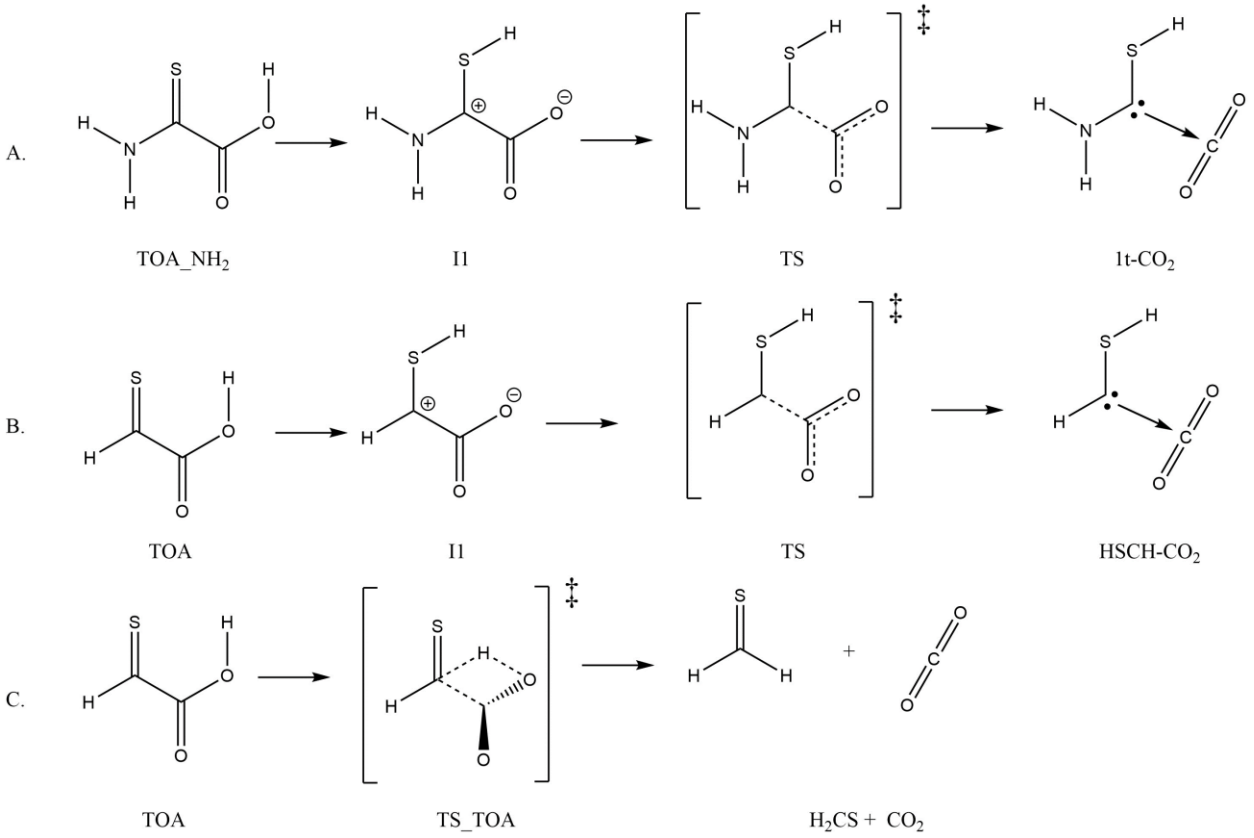

Scheme 3. A. Decomposition of TOA_NH_2 according to Bernhardt et al. [56]; B. Assumed decomposition of TOA, following the same proposal as in reference [56]; C. Actual decomposition of TOA according to the transition state found in this study.

Formation of the intermediate zwitterion I1 is unfavoured with respect to a direct transfer of the hydrogen atom from oxygen to carbon, leading to dissociation into H_2CS and CO_2 through the transition state TS_TOA, also shown in Figure 7. At the jChS level, HSCH-CO_2 (the analogue of 1t-CO_2) was found to be 35.6 kcal mol^{-1} over TOA, while the decomposition product (H_2CS and CO_2) is -8.5 below TOA, and -50.7 kcal mol^{-1} below acetylene and SO_2. The barrier for this transformation is 27.1 kcal mol^{-1}, significantly lower than the barrier needed to overcome TSiso_11. Since the reverse transformation from H_2CS and CO_2 has a larger barrier than that needed for the direct decomposition, it is probable that the product of the whole cycloaddition reaction of SO_2 to acetylene is $H_2C{=}S$ and CO_2. This process has therefore been included in the scheme in Fig. 4 and the PES in Fig.5.

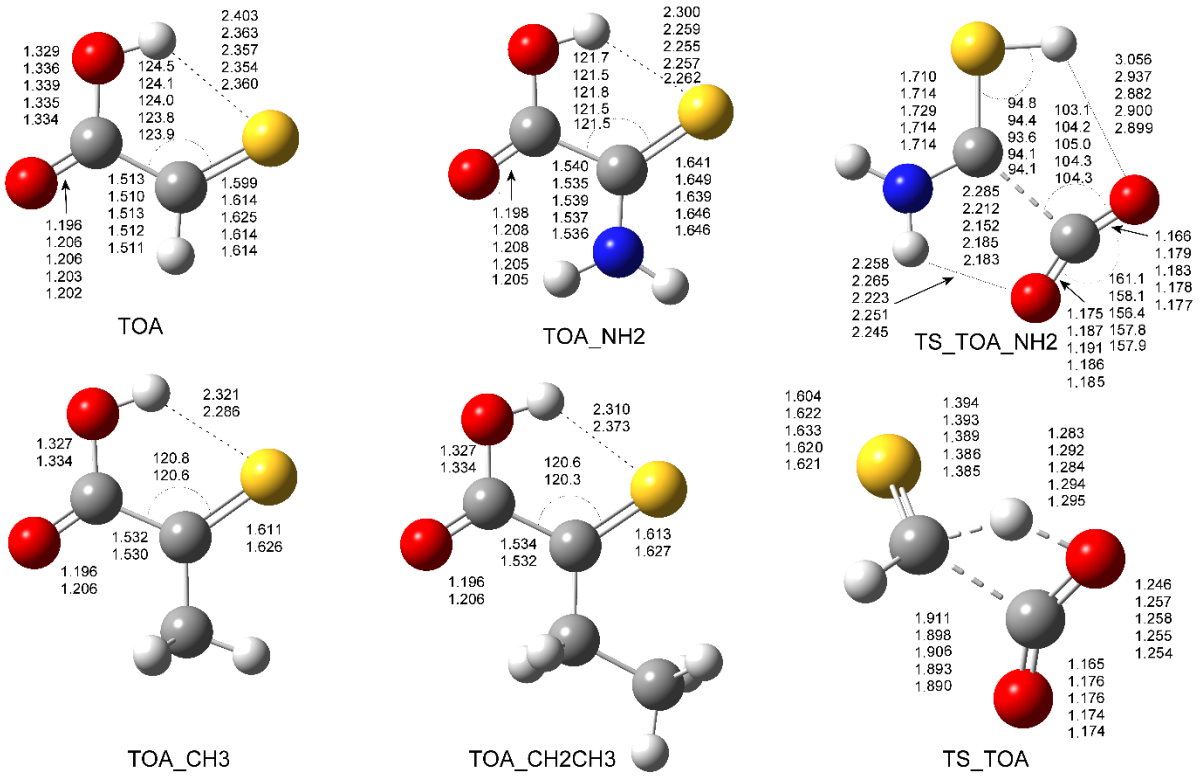

Figure 7. Structure of the parent TOA and the amino, methyl and ethyl derivatives. Distances in Å and angles in degrees. From top to bottom, the entries refer to geometries at the M06-2X-D3/jun-cc-pV(T+*d*)Z, revDSD-PBEP86-D3(BJ)/jun-cc-pV(T+*d*)Z, CCSD(T)/cc-pVTZ, CCSD(T)-F12/cc-pVDZ-F12, and CCSD(T)-F12/cc-pVTZ-F12. The highest-level of calculations (CCSD(T)-F12/cc-pVTZ-F12) was performed only for the smallest molecules. CCSD(T)/cc-pVTZ calculations for TOA_NH_2 and the corresponding transition state were taken from reference [56].

The structure of the transition state found in reference [56] for TOA_NH_2 was re-optimized with the methods used in the present study and the computed geometrical parameters are given in Figure 7. The agreement among the methods is not so close for the TSs as it is for the stable species. Looking at the C···C and H···O distances in TS_TOA_NH_2, the transition state optimized at the DFT levels is looser than that optimized at the CCSD(T)/cc-pVTZ level. In turn, the latter is slightly tighter than the structure obtained at the more accurate CCSD(T)-F12/cc-pVTZ-F12 level. A similar trend can be observed for TS_TOA. It remains to be seen whether the reactions of the other two alkyl-substituted species follow mechanism A or C of Scheme 3.

3.4. Confirming the concerted [3+2] addition of SO_2 to acetylene

The last part of this work is devoted to the study of the structure of the transition state governing the [3+2] cycloaddition of SO_2 to acetylene with a larger panel of methods and basis sets than in our previous work[4], in order to verify if the generally accepted concerted mechanism is preferred or not. Figure 8 shows the structure of the envelope-like transition state TS2A and Table 4 shows selected geometrical parameters using different wavefunction and DFT methods.

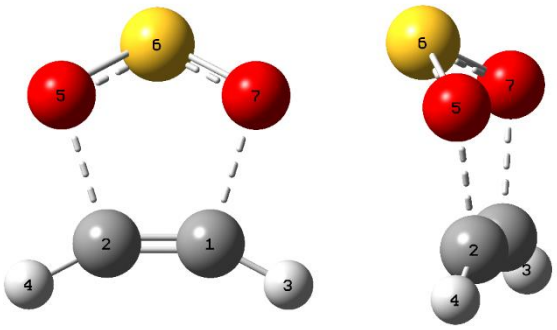

Figure 8. Head-on and side views of the structure of the transition state TS2A governing the reaction between sulfur dioxide and acetylene. Atom labelling is also reported to identify the geometrical parameters given in Table 4.

It is worth pointing out at this point a study performed by Karton and Goerigk[57] on pericyclic reactions and another one by Yu et al.[58] where they studied the barrier heights for the cycloreversion of heterocyclic rings (the opposite reactions to cyclization). In both papers, they examined the performance of different DFT[59] methods and, not surprisingly, they found that double-hybrid functionals (e.g. DSD-PBEP86-D3)[24] delivered the best results in comparison with high-level composite methods.[60] Obviously, there are many more DFT methods[61] that could be used to perform the geometry optimizations presented in Table 4, but, in our opinion, the selected approaches are representative of the most sophisticated and accurate models currently available.

The data presented show that the DSD-PBEP86 method reproduces the symmetric structure of the TS provided by all the other methods (resulting in identical values of the R(17) and R(25) geometrical

parameters) with the aug- and jun-cc-pV(T+*d*)Z basis sets, both including or neglecting dispersion contributions. The non-symmetric structure appears only when the def2-TZVPP or jun-cc-pV(Q+*d*)Z basis sets are employed. On the other hand, the revised version of the method (revDSD-PBEP86)[18] reproduces the correct symmetrical structure, again when combined with the aug- and jun-cc-pV(T+*d*)Z basis sets, but only when dispersion contributions are excluded. Neither B3LYP (used for the geometry optimization by some wavefunction composite methods), nor M06-2X[23] or the B2PLYP[25] double-hybrid functional exhibit this inconsistency, irrespective of the selected basis set. An explanation could be attempted based on the double hybrid character of revDSD-PBEP86, i.e., that the error comes from the introduction of MP2 in the correlation functional. However, neither pure MP2 calculations by themselves, nor the other double-hybrid B2PLYP functional exhibit this behavior. For this reason, another explanation may be sought into the possible instabilities caused by the different weights of MP2 and DFT correlation for parallel and anti-parallel spins.

It is also interesting to compare the results obtained by different wavefunction methods. At the MP2 and MP2-F12 levels, the C–O bonds are considerably shorter than those obtained at the higher CCSD(T) or CCSD(T)-F12 levels. They are also noticeably shorter than the bond lengths obtained at the B3LYP, M06-2X or B2PLYP levels, while they are close to those obtained at the revDSD-PBEP86 level, with this trend suggesting a non-optimal mixing of MP2 and DFT correlation in the parametrization of this functional. Basis set extension decreases one of the C-O bond lengths (that becomes even shorter than its MP2 counterpart) and increases the other one for both the original and revised versions of DSD-PBEP86. This trend increases the asymmetry of the TS structure, leading to a non-concerted mechanism in place of the concerted one suggested by the more accurate CCSD(T) or CCSD(T)-F12 methods.

Table 4. Bond distances (in Å) between atoms in the optimized structures of TS2A obtained at different levels of theory. Numbering of the atoms as shown in Fig. 8.

Method	Basis Set	R(12)	R(13)	R(24)	R(17)	R(25)	R(56)	R(67)
B3LYP	6-311G(2d,d,p)[a]	1.255	1.068	1.068	1.882	1.882	1.545	1.545
	cc-pV(T+d)Z[b]	1.253	1.066	1.066	1.874	1.874	1.534	1.534
M06-2X-D3	jun-cc-pV(T+d)Z	1.247	1.067	1.067	1.884	1.884	1.513	1.513
	jun-cc-pV(Q+d)Z	1.246	1.066	1.066	1.881	1.881	1.510	1.510
	aug-cc-pV(T+d)Z	1.247	1.067	1.067	1.884	1.884	1.513	1.513
revDSD-PBEP86-D3(BJ)	*jun-cc-pV(T+d)Z*	*1.264*	*1.070*	*1.068*	*1.772*	*1.931*	*1.528*	*1.547*
	jun-cc-pV(Q+d)Z	*1.262*	*1.070*	*1.067*	*1.750*	*1.950*	*1.522*	*1.546*
	aug-cc-pV(T+d)Z	*1.263*	*1.070*	*1.068*	*1.798*	*1.902*	*1.532*	*1.545*
	def2-TZVPP	*1.265*	*1.071*	*1.067*	*1.720*	*1.996*	*1.520*	*1.554*
revDSD-PBEP86	jun-cc-pV(T+d)Z	1.263	1.069	1.069	1.849	1.849	1.538	1.538
	jun-cc-pV(Q+d)Z	*1.261*	*1.069*	*1.068*	*1.838*	*1.854*	*1.534*	*1.536*
	aug-cc-pV(T+d)Z	1.263	1.069	1.069	1.850	1.850	1.539	1.539
	def2-TZVPP	*1.263*	*1.070*	*1.068*	*1.771*	*1.919*	*1.528*	*1.546*
DSD-PBEP86-D3(BJ)	jun-cc-pV(T+d)Z	1.263	1.069	1.069	1.842	1.842	1.537	1.537
	jun-cc-pV(Q+d)Z	*1.261*	*1.068*	*1.068*	*1.811*	*1.867*	*1.531*	*1.537*
	aug-cc-pV(T+d)Z	1.263	1.069	1.069	1.842	1.842	1.538	1.538
	def2-TZVPP	*1.263*	*1.070*	*1.068*	*1.771*	*1.918*	*1.528*	*1.546*
DSD-PBEP86	jun-cc-pV(T+d)Z	1.263	1.069	1.069	1.842	1.842	1.537	1.537
	jun-cc-pV(Q+d)Z	*1.261*	*1.068*	*1.068*	*1.811*	*1.867*	*1.531*	*1.537*
	aug-cc-pV(T+d)Z	1.263	1.069	1.069	1.842	1.842	1.537	1.537
	def2-TZVPP	*1.263*	*1.070*	*1.068*	*1.771*	*1.919*	*1.528*	*1.546*
B2PLYP-D3(BJ)	jun-cc-pV(T+d)Z	1.261	1.066	1.066	1.844	1.844	1.543	1.543
	jun-cc-pV(Q+d)Z	1.270	1.066	1.066	1.841	1.841	1.540	1.540
	aug-cc-pV(T+d)Z	1.261	1.066	1.066	1.845	1.844	1.544	1.544
MP2	jun-cc-pV(T+d)Z	1.269	1.068	1.068	1.807	1.807	1.544	1.544
	jun-cc-pV(Q+d)Z	1.266	1.067	1.067	1.802	1.802	1.539	1.539
	aug-cc-pV(T+d)Z	1.269	1.068	1.068	1.807	1.807	1.545	1.545
CCSD(T)	jun-cc-pV(T+d)Z	1.266	1.069	1.069	1.878	1.878	1.537	1.537
	aug-cc-pV(T+d)Z	1.266	1.069	1.069	1.878	1.878	1.538	1.538
MP2-F12	cc-pVDZ-F12	1.265	1.067	1.067	1.801	1.801	1.537	1.537
	cc-pVTZ-F12	1.265	1.067	1.067	1.799	1.799	1.536	1.536
CCSD(T)-F12	cc-pVDZ-F12	1.263	1.068	1.068	1.865	1.865	1.529	1.529
	cc-pVTZ-F12	1.262	1.068	1.068	1.867	1.867	1.529	1.529

[a] Basis set used in the B3LYP geometry optimization embedded in the CBS-QB3 method. [b] Basis set used in the B3LYP geometry optimization embedded in the W1BD method.

4. CONCLUSIONS

Following our recent study of the [3+2] addition of SO_2 to ethylene and acetylene, we report in the present paper the main results of a comprehensive quantum chemical analysis of the [2+2] and [2+1] additions. We used DFT and composite wavefunction methods to determine the possible reaction mechanisms and found out a rich set of reactions arising from 2B, the main product resulting from the [2+2] cycloaddition of SO_2 to acetylene.

The cyclic 1,2-oxathietane 2-oxide, 2B, opens toward one of the conformers of sulfinyl acetaldehyde, saSA, in equilibrium with the other three possible isomers. Several isomerization and decomposition reactions are possible for these isomers. The most probable path leads from the asSA isomer (lying 16.3 kcal mol^{-1} below the reactants) toward ethenone 1-(SO)-thioperoxol, ETP, which has about the same

energy. ETP, in turn, can rearrange to 2-thioxoacetic acid (TOA), which is 42.2 kcal mol^{-1} more stable than the reactants. Finally, TOA can decompose to CO_2 + H_2C=S, whose combined energy is 50.7 kcal mol^{-1} below that of the reactants. The barrier for such a transformation is very high (69.3 kcal mol^{-1}) but the corresponding transition state, TSdec_4, lies 17 kcal mol^{-1} below TS2B, the transition state involved in the formation of 2B. Thus, if 2B is formed, the system has more than enough excess energy to arrive at this decomposition product. Then, the global reaction representing the process would be:

$$SO_2 + HC{\equiv}CH \rightarrow CO_2 + H_2C{=}S, \qquad \Delta(E+ZPE) = -50.7 \text{ kcal mol}^{-1}$$

with all relevant TSs lying below the initial one, TS2B.

We studied in more detail the decomposition of TOA, on the one side because we did not find previous theoretical or experimental studies on TOA itself, and on the other side because of a recent experimental and theoretical study of 2-amino-2-thioxoacetic acid TOA_NH_2, performed by Bernhardt et al. [56] We found that the transition states for the decomposition of TOA and TOA_NH_2 are different, corresponding in the first case to a corkscrew rotation of the OCO moiety with a concomitant H-transfer from the acidic oxygen directly to the sulfur-bearing carbon atom. This contrasts the process described in reference [56], which involves a zwitterion formed by the H-transfer from oxygen to sulfur, followed by the breaking of the C-C bond, which generates a singlet carbene species and CO_2. Our results suggest that it would be interesting to understand how the substituent on C2 affects the process of decomposition, whether both transition states are possible, or alternatively, whether the decomposition of the parent species is a unique event.

ACKNOWLEDGMENTS

ZS, NR, and NT thank the STARK group for the high-performance computing facilities and Scuola Normale Superiore for financial support through the project "Computational Modeling for Environmental Chemistry and Sustainability: from atmospheric monitoring to photo-catalysis". The research of NR has been performed during and with the support of the Italian inter-university Ph.D. course in sustainable development and climate change (link: www.phd-sdc.it). One of the authors (O.N.V.) acknowledges the continuing support to his research by the National Agency for Research and Innovation (ANII) and the Program for the Support of Basic Sciences (Pedeciba) from Uruguay. One of the authors (V.B.) thanks Gaussian Inc. for a R&D grant.

REFERENCES

[1] P. Quadrelli, *Modern Applications of Cycloaddition Chemistry*, Elsevier Inc. (ISBN: 9780128152737) **2019**.

[2] D. Svatunek, R. P. Pemberton, J. L. Mackey, P. Liu, K. N. Houk, *J. Org. Chem.* **2020**, *85*, 3858.

[3] M. V. Panova, M. G. Medvedev, M. A. Mar'yasov, K. A. Lyssenko, O. E. Nasakin, *J. Org. Chem.* **2021**, *86*, 4398.

[4] Z. Salta, M. Vega-Teijido, A. Katz, N. Tasinato, V. Barone, O. N. Ventura, *J. Comput. Chem.* **2022**, *43*, 1420.

[5] J. F. Liebman, K. N. Petersen, P. N. Skancke, *Acta Chem. Scand.* **1999**, *53*, 1003.

[6] Y. Lan, S. E. Wheeler, K. N. Houk, *J. Chem. Theory Comput.* **2011**, *7*, 2104.

[7] L. A. Carpino, L. V. III McAdams, R. H. Rynbrandt, J. W. Spiewak, *J. Am. Chem. Soc.* **1971**, *93*, 476.

[8] L. A. Carpino, J. R. Williams, *J. Org. Chem.* **1974**, *39*, 2320.

[9] J. A. Jr. Montgomery, M. J. Frisch, J. W. Ochterski, G. A. Petersson, *J. Chem. Phys.* **1999**, *110*, 2822.

[10] J. A. Jr. Montgomery, M. J. Frisch, J. W. Ochterski, G. A. Petersson, *J. Chem. Phys.* **2000**, *112*, 6532.

[11] A. D. Becke, *J. Chem. Phys.* **1993**, *98*, 5648.

[12] J. M. L. Martin, G. de Oliveira, *J. Chem. Phys.* **1999**, *111*, 1843.

[13] S. Parthiban, J. M. L. Martin, *J. Chem. Phys.* **2001**, *114*, 6014.

[14] E. C. Barnes, G. A. Petersson, J. A. Jr. Montgomery, M. J. Frisch, J. M. L. Martin, *J. Chem. Theor. Comput.* **2009**, *5*, 2687.

[15] S. Alessandrini, V. Barone, C. Puzzarini, *J. Chem. Theory Comput.* **2020**, *16*, 988.

[16] J. Lupi, S. Alessandrini, C. Puzzarini, V. Barone, *J. Chem. Theory Comput.* **2021**, *17*, 6974.

[17] V. Barone, J. Lupi, Z. Salta, N. Tasinato, *J. Chem. Theory Comput.* **2021**, *17*, 4913.

[18] G. Golokesh Santra, N. Sylvetsky, J. M. L. Martin, *J. Phys. Chem. A.* **2019**, *123*, 5129.

[19] N. C. Handy, J. A. Pople, M. Head-Gordon, K. Raghavachari, G. W. Trucks, *Chem. Phys. Lett.* **1989**, *164*, 185.

[20] T. Helgaker, W. Klopper, H. Koch, J. Noga, *J. Chem. Phys.* **1997**, *106*, 9639.

[21] C. Møller, M. S. Plesset, *Phys. Rev.* **1934**, *46*, 618.

[22] R. J. Bartlett, G. D. Purvis, *Int. J. Quantum Chem*. **1978**, *14*, 561.

[23] Y. Zhao, D. G. Truhlar, *Theor Chem. Acc.* **2008**, *120*, 215.

[24] S. Kozuch, J. M. L. Martin, *Phys. Chem. Chem. Phys.* **2011**, *13*, 20104.

[25] S. Grimme, *J. Chem. Phys.* **2006**, *124*, No. 034108.

[26] H.-J. Werner, T. B. Adler, *J. Chem. Phys.* **2007**, *12*6, 164102.

[27] G. Knizia, T. B. Adler, H.-J. Werner, *Chem. Phys.* **2009**, *130*, 054104.

[28] R. A. Kendall, T. H., Jr. Dunning, R. J. Harrison, *J. Chem. Phys.* **1992**, *96*, 6796.

[29] E. Papajak, J. Zheng, X. Xu, H. R. Leverentz, D. G. Truhlar, *J. Chem. Theory Comput.* **2011**, *7*, 3027.

[30] F. Weigend, R. Ahlrichs, *Phys. Chem. Chem. Phys.* **2005**, *7*, 3297.

[31] S. Grimme, J. Antony, S. Ehrlich, H. Krieg, *J. Chem. Phys.* **2010**, *132*, 154104.

[32] Z. Salta, M. E. Segovia, A. Katz, N. Tasinato, V. Barone, O. N. Ventura, *J. Org. Chem.* **2021**, *86*, 2941.

[33] V. Barone, G. Ceselin, M. Fusè, N. Tasinato, *Front. Chem.* **2020**, *2*, 584203.

[34] K. A. Peterson, T. B. Adler, H.-J. Werner, *J. Chem. Phys.* **2008**, *128*, 84102.

[35] J. G. Hill, K. A. Peterson, *Phys. Chem. Chem. Phys.* **2010**, *12*, 10460.

[36] J. G. Hill, K. A. Peterson, *J. Chem. Phys.* **2014**, *141*, 094106.

[37] K. Fukui, *Acc. Chem. Res.* **1981**, *14*, 363.

[38] F. Weinhold, J. E. Carpenter, *The Natural Bond Orbital Lewis Structure Concept for Molecules, Radicals, and Radical Ions, and references therein*, in Naaman, R., Vager, Z. (eds) *The Structure of Small Molecules and Ions*. Springer, Boston, MA., pp. 227–236, **1988**.

[39] Gaussian 16, Revision C.01, M. J. Frisch, G. W. Trucks, H. B. Schlegel, G. E. Scuseria, M. A. Robb, J. R. Cheeseman, G. Scalmani, V. Barone, G. A. Petersson, H. Nakatsuji, X. Li, M. Caricato, A. V. Marenich, J. Bloino, B. G. Janesko, R. Gomperts, B. Mennucci, H. P. Hratchian, J. V. Ortiz, A. F. Izmaylov, J. L. Sonnenberg, D. Williams-Young, F. Ding, F. Lipparini, F. Egidi, J. Goings, B. Peng,

A. Petrone, T. Henderson, D. Ranasinghe, V. G. Zakrzewski, J. Gao, N. Rega, G. Zheng, W. Liang, M. Hada, M. Ehara, K. Toyota, R. Fukuda, J. Hasegawa, M. Ishida, T. Nakajima, Y. Honda, O. Kitao, H. Nakai, T. Vreven, K. Throssell, J. A. Montgomery, Jr., J. E. Peralta, F. Ogliaro, M. J. Bearpark, J. J. Heyd, E. N. Brothers, K. N. Kudin, V. N. Staroverov, T. A. Keith, R. Kobayashi, J. Normand, K. Raghavachari, A. P. Rendell, J. C. Burant, S. S. Iyengar, J. Tomasi, M. Cossi, J. M. Millam, M. Klene, C. Adamo, R. Cammi, J. W. Ochterski, R. L. Martin, K. Morokuma, O. Farkas, J. B. Foresman, and D. J. Fox, Gaussian, Inc., Wallingford CT, **2016**.

[40] MOLPRO, version 19.1, a package of ab initio programs, H.-J. Werner, P. J. Knowles, G. Knizia, F. R. Manby, M. Schütz, and others, see https://www.molpro.net. **2020**.

[41] T. Durst, B. P. Gimarzevsky, *J. Chem. Soc.: Chem. Commun.* **1975**, 724.

[42] M. D. Gray, D. R. Russell, D. J. H. Smith, T. Durst, B. Gimbarzevsky, *J. Chem. Soc. Perkin Trans.* **1981**, *1*, 1826.

[43] L. Breau, N. K. Sharma, I. R. Butler, T. Durst, *Can. J. Chem.* **1991**, *69*, 185.

[44] O. B. Bondarenko, L. G. Saginova, N. V. Zyk, *Russ. Chem. Rev.* **1996**, *65*, 147.

[45] P. Johnson, R. J. K. Taylor, *Tetrahedron Lett.* **1997**, *38*, 5873.

[46] T. Harel, E. Amir, S. Rozen, *Org. Lett.* **2006**, *8*, 1213.

[47] Y. Nakano, S. Saito, Y. Morino, *Bull. Chem. Soc. Japan* **1970**, *43*, 368.

[48] H.-L. Hase, C. Müller, A. Schweig, *Tetrahedron* **1978**, *34*, 3983.

[49] P. Pflieger, C. Mioskowski, J. P. Salaun, D. Weissbart, F. Durst, *Tetrahedron Lett.* **1988**, *29*, 6775.

[50] M. M. Cifuentes García, J. L. García Ruano, A. M. Martín Castro, J. H. Rodríguez Ramos, I. Fernández, *Tetrahedron: Asymm.* **1998**, *9*, 859.

[51] J. L. García Ruano, J. Alemán, M. B.Cid, M. Á. Fernández-Ibáñez, M. C. Maestro, M. R. Martín, A. M. Martín-Castro, *Asymmetric Transformations Mediated by Sulfinyl Groups*, in Organosulfur Chemistry in Asymmetric Synthesis, T. Toru, C. Bolm (eds), Wiley-VCH, Heidelberg, pp. 55–106 **2008**.

[52] M. Stipanuk, *Ann. Rev. Nutr.* **1986**, *6*, 179.

[53] R. Annunziata, M. Cinquini, F. Cozzi, *J. Chem. Soc., Perkin Trans.* **1979**, *1*, 1687.

[54] Z. Salta, N. Tasinato, O. N. Ventura, J. F. Liebman, *Struct. Chem.* **2023**, *34*, 723.

[55] O. N. Ventura, M. E. Segovia, M. Vega–Teijido, A. Katz, M. Kieninger, N. Tasinato, Z. Salta, *J. Phys. Chem. A* **2022**, *126*, 6091.

[56] B. Bernhardt, M. Schauermann, E. Solel, A. K. Eckhardt, P. R. Schreiner, *Chem. Sci.* **2023**, *14*, 130.

[57] A. Karton, L. Goerigk, *J. Comput. Chem.* **2015**, *36*, 622.

[58] L.-J. Yu, F. Sarrami, R. J. O'Reilly, A. Karton, *Chem. Phys.* **2015**, *458*, 1.

[59] A. M. Teale, T. Helgaker, A. Savin, C. Adamo, B. Aradi, A. V. Arbuznikov, P. W. Ayers, E. J. Baerends, V. Barone, P. Calaminici et al., *Phys. Chem. Chem. Phys.* **2022**, 24, 28700.

[60] A. Karton, *Annual Reports in Computational Chemistry* **2022**, *18*, 123.

[61] N. Mehta, T. Fellowes, J. M. White, L. Goerigk, *J. Chem. Theory Comput.* **2021**, *17*, 2783.